2021 IEEE PES/IAS PowerAfrica

Investigation and Characterization of Al paste as back surface field (BSF) for High Efficiency Si Solar cell

Michael A. Awaah
Dept. of Electrical Engineering, CSET, Grand Canyon University
Phoenix, AZ USA
awaahm@yahoo.com

Isibhakhomen Awaah
Intel Corporation
Chandler, AZ, USA,
blackisi@yahoo.com

Vitus A. Apalangya
Dept. of Food Process Engineering, School of Engineering, University of Ghana, Legon
Accra, Ghana,
vapalangya@gmail.com

Kumar K. Das
Dept. of Electrical Engineering, Tuskegee University
Tuskegee Al USA
kdas111@gmail.com

Abstract **– Photovoltaic solar cells offer many advantages, including needing little maintenance, environmentally benign of any electricity generating source with zero greenhouse gas emission. In the photovoltaic industry both the reduction of the silicon material thickness and the increase of the solar cells efficiency are critical topics for cost reduction. One key factor to reducing the cost and energy consumption of solar cell production process is reducing the thickness of the Si wafer to the order of 200 µm, the current industry wafer thickness ranges of 275 - 350 µm. The back-surface field (BSF), ~50 µm thick is formed during the firing of a screen printed A1 on the rear side. The main issue using thinner wafers with Al BSF is the bow of the wafers after firing.**

In this study, baseline Si Solar cells with 19.7% light conversion efficiencies was achieved on monocrystalline p-type CZ-Si with two types of Al BSF pastes. High performance SiN:H was grown by PECVD tool. The Al/Ag firing process for the Sun Chemical product (CTX 0435) needs to be optimized as the current process disintegrates to powder substance after Ag firing. The process window for firing the DuPont Ag front-side paste is large and yields low series resistance values without forming gas anneal (FGA anneal).

Keywords: High Efficiency Si Solar Cell, Si solar cell using Al back surface field, Back surface field (BSF), Al-BSF formation, rear surface passivation.

I. INTRODUCTION

Major issues affecting the manufacturing photovoltaic modules include technological advances, improved production methods, dramatically lower prices for PV modules.

The cost of manufacturing Silicon solar cell can be significantly lowered using thinner wafers, ~180 µm thick [1]. However, thin wafers are susceptible to bowing caused by the influence of the metallization on the front and rear side. Excessive bowing of Si wafers leads to significant yield losses during production process. In this investigation, custom-made formulations that combines good doping conductive aluminum paste was designed to deliver excellent efficiency, low bowing, high material compatibility, better adhesion strength and a wider processing window.

Photovoltaic cells of single-junction can be categorized as wafer-based, thin films, and emerging technologies. A typical crystalline solar cell architecture consists of a p-type substrate with n and p-metal contacts at the backside as shown in Figure 1.

The internal structure of a solar cell has a p-n junction formed between the n-doped emitter and the p-doped. The front surface is textured and coated with an antireflection coating (ARC) layer to enhance the light absorption. The ARC also provides passivation to the front side to decrease front surface recombination velocity (FSRV). Silver (Ag) front grid forms the front contact.

Solar cells that possess full metal/Si interface at their rear surface field have low cell efficiency i.e., less than 20%) [2]. Boron (B) diffusion is an attractive method for achieving high-quality rear interface. Boron diffusion usually uses liquid BBr_3 [3], BCl_3 [4], or solid B [5] as the source of B. Considerable efforts have been made recently to develop an industrially feasible approach for B diffusion, with liquid BBr_3 and Si paste as the source. However, BBr_3 is
hazardous and requires an extra laser equipment to allow diffusion, hence increasing the cost of production.

In this work presented, new low-cost improved paste [6] with low sheet resistance was used to achieve solar cell with reasonable conversion efficiency. The method requires printing machine where patterns are controlled by selecting appropriate paste and screen. Du et al. [7] prepared Al/B paste and demonstrated a high doping concentration in the BSF by B doping.

The back-surface field (BSF) formed by the Al alloyed with the substrate reduces recombination at the back side and improves the open-circuit voltage (V_{oc}).

978-1-6654-0311-5/21/$31.00 ©2021 IEEE

2021 IEEE PES/IAS PowerAfrica | 978-1-6654-0311-5/21/$31.00 ©2021 IEEE | DOI: 10.1109/POWERAFRICA52236.2021.9543257

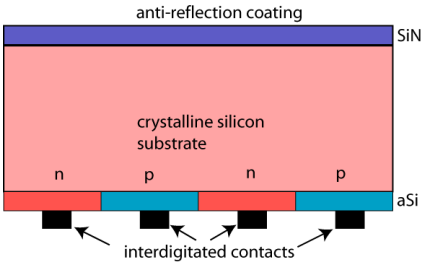

Figure 1: Standard silicon solar cell structure with contacts and antireflection coating.

Under illumination, electron-hole pairs are first created in the absorber layer by the absorption of incident photons, which transfer their energy to loosen electrons, knocking them off Si atoms. Then electrons as minority carriers diffuse to the space charge region and are swept across the junction by the electric field at the depletion region to reach the n-type emitter, where they become majority carriers. The photo-generated current then flows through the external circuit if the front and rear metal electrodes are connected together. The critical parameters which determine the efficiency of a solar cell are the product of short-circuit current (J_{sc}), open-circuit voltage V_{oc} and fill factor (FF), Figure 2.

The major types of Solar cell absorber material are crystalline and thin films [1], [8], which vary from each other in terms of light absorption efficiency, energy conversion efficiency, manufacturing technology and cost of production. Single crystalline silicon cells are the most common in the PV industry.

The main technique for producing single crystal silicon is the Czochralski (CZ) method in which high-purity polycrystalline silicon is melted in a quartz crucible [9]. A single-crystal silicon seed is dipped into this molten mass of polycrystalline silicon. As the seed is pulled slowly from the melt, a single-crystal ingot is formed. The ingots are then sawed into thin wafers, polished, doped, coated, interconnected and assembled into modules and arrays.

Prime quality p-type CZ (100) Si wafers from Si QESST were employed and processed using standard baseline Si flow. In this investigation, state of the art front side nitride layer was deposited to the rear side with a thin thermal oxide layer to improve the inversion layer [10]. Key to improving the efficiency of a crystalline cell is reducing the thickness of the Si wafer, fine tuning firing recipe, reduce shading loss, increase J_{sc}, V_{oc}.

One way of decreasing the shading is the use of narrower gridlines. In order to benefit from the narrow gridlines even with many breakages, multiple busbars can be introduced, this also leads to the reduction of gridline resistance and improve the FF.

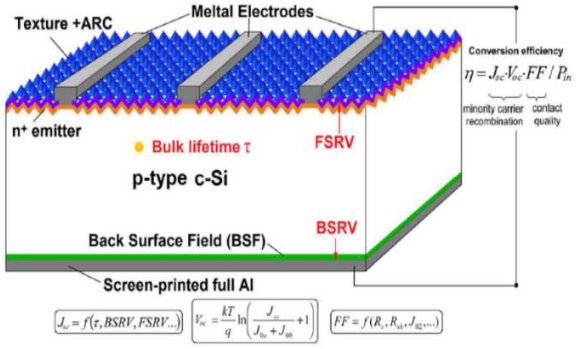

Figure 2: Standard solar cell structure showing top and back contacts, passivation, ARC coating, surface fields and cell characterization parameters.

Figure 3: Design patterns with different number of busbars

Figure 3: Design patterns with different number of busbars

II. METHODOLOGY

The fabrication of Al-BSF cell involves emitter formation, deposition of ARC layer of SiNx, front and bac
As
with 1 Ωcm resistivity from Si QESST were employed and processed using standard baseline Si flow. The wafers went through initial saw-damage removal and surface texturing processing to increase the optical absorption by randomizing the incident light [11]. Anisotropic texturing of the Cz-Si material was achieved in alkaline solutions such as KOH [12 -13], which lead to the formation of random pyramids on the silicon surface. To reduce the surface roughness and its impact on the effective charge carrier lifetime, the rear surface was polished.

After $POCl_3$ diffusion, all wafers received passivation from the nitride film deposition tool. The deposition of the dielectric layer was completed during the passivation step. The solar cells were designed, fabricated and optimized for best performance by minimizing series resistance and rear surface recombination.

Half the wafers were coated with Al BSF paste from Sun Chemical while the other half coated with Al paste from DuPont chemicals. At the Al firing step, three of the wafers (one coated with Sun Chemical Al paste and other two coated with DuPont Al paste) received the baseline (pyro temp 826, 836, 846ºC for 30 s) while the other three were fired with a different recipe received

978-1-6654-0311-5/21/$31.00 ©2021 IEEE

temperatures 790, 795, 799ºC for 3 s). The peak firing temperature for the Ag paste was 715ºC. All six wafers had good adhesion on the front side Ag grid and back side Al after Al firing process.

The contact formation and current transport mechanisms for the screen-printed contacts were reviewed to understand the impact of contact co-firing on solar cell performance.

The fabricated solar cells were fired with original CXT-0435 Al recipe with a peak temperature of 797°C and a ~3.8 s ramp from 450 - 785°C prior to stabilizing. The wafer looked good after firing. After Ag firing, began to bubble and disintegrate everywhere. An average sheet resistance (Rs_{avg}) values of 0.98 Ω-cm^2 was recorded.

Three of the wafers received a post process forming gas anneal (FGA) for 20 minutes at 400ºC, in MRL furnace. Flash test and Electroluminescence (EL) measurements were collected before and after the FGA treatment

III. RESULTS AND DISCUSSIONS

Baseline Si solar cells was fabricated and investigated using two types of Al BSF pastes for front side metallization. Reasonable minority carrier lifetime values (~30 µs) was measured after $POCl_3$ diffusion and after silicon nitride arc layer deposition, as shown in Figure 4. The lifetime values look reasonably unchanged.

Figures 5 shows an optical plot of refractive index (*n*) and extinction coefficient (k) vs. wavelengths (λ) of light for the 78nm thick amorphous hydrogenated silicon nitride(a-SiNx:H) deposited with a PECVD tool. The data was acquired by variable angle spectroscope ellipsometry (VASE). The k values remained unchanged with an increase in *n* parameter after firing.

Rutherford back scattering (RBS) data was collected and summarized in Table 1 for pre- and post-firing for silicon nitride. The target composition of Si:N:H after deposition was 40:42:18. After firing, N composition increased while the H composition reduced in the arc layer.

Table 2 and 3 summarizes I-V measurement (V_{oc}, J_{sc}, FF and efficiencies) collected for SPL Lot 15 before and after FGA treatment.

Flash tests showed reasonable solar cells conversion efficiencies (η %) ranging from 18.7 – 19.7%, low series resistance (0.55 – 1.30 Ω-cm^2), except for SPL-0091 which recorded high series resistance of 1.8 Ω-cm^2, this does not suggest any contact resistance problem. Open circuit voltage, V_{oc} of ~640 mV was measured, this was consistent in all the cells with an average Fill Factor (FF) of 78% recorded. Though several of the cells disintegrated with powdered substance everywhere, no degradation in cell performance was observed.

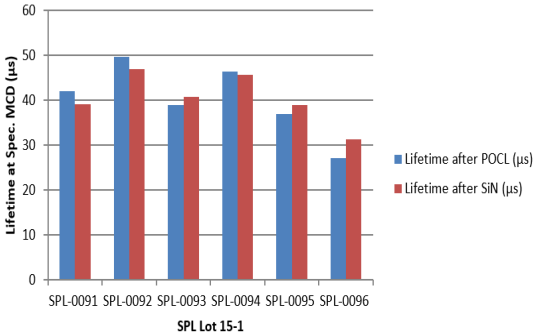

Figure 4: Lifetime measurement (MCD = 1.0x 10^{14} /cm^3).

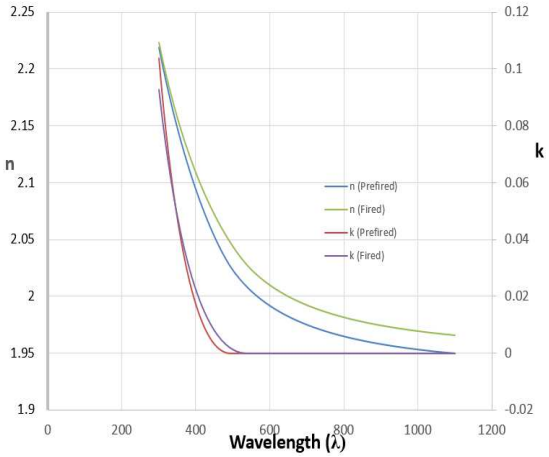

Figures 5: Refractive index (*n*) and extinction coefficient (k) vs. wavelengths (λ) of light for the 78nm amorphous hydrogenated silicon nitride(a-SiNx:H)

Table 1: RBS data for CSSER Oxford amorphous

Sample	Si	N	H
Unfired	38.9	43.3	17.8
Fired	41.0	46.5	12.5

Table 2. I-V performance results of SPL Lot 15 cells

Wafer ID	V_{oc} (mV)	FF (%)	J_{sc} (mA/cm^2)	η (%)	R_s (Ω-cm^2)	BSF thickness (µm)
SPL-0091	644	78.7	38.9	19.72	1.8	6.3
SLP-0092	645	78.9	37.5	19.08	0.68	6.9
SPL-0093	642	79.3	38.3	19.50	0.55	5.19
SPL-0094	640	78.1	37.9	18.94	1.3	6.4
SPL-0095	638	78.9	38.2	19.23	0.89	6.1
SPL-0096	635	79.1	37.6	18.89	0.65	5.8

978-1-6654-0311-5/21/$31.00 ©2021 IEEE

Three of the wafers received a post process forming gas anneal (FGA- 95% nitrogen and 5 % hydrogen) treatment for 20 minutes at 400 °C in MRL furnace. Most of the parameters remained
unchanged. The two other cells, SPL-0092 and 0096 with low series resistances pre-FGA treated saw an increase in series resistances and degrade efficiencies. The reasons for these increases are currently not understood.
For the SPL-0092 cell, a microscope inspection showed evidence of broken grid connected to busbar (broken fingers).
Electroluminescence (EL) images are summarized in Figures 6 and 7.
Quantum efficiency (QE) analysis of the cells, which measures the ratio of the number of carriers collected by the solar cell to the number of photons of a given energy incident the solar cell revealed good cell with EQE conversion efficiencies of above 90% in the 660 and 690 nm wavelength range.

Table 3: I-V performance results of SPL Lot 15 cells after FGA treatment

Wafer ID	Voc (mV)	FF (%)	J_{sc} (mA/cm^2)	η (%)	R_s (Ω-cm^2)	BSF thickness (µm)
SPL-0091	644	78.7	38.9	19.72	1.8	6.3
SLP-0091 FGA	632	76.4	38.7	18.69	1.65	6.3
SLP-0092	645	78.9	37.5	19.08	0.68	6.9
SPL-0092 FGA	643	76.9	37.3	18.44	1.35	6.9
SPL-0096	642	79.3	38.3	19.50	0.55	5.19
SPL-0096 FGA	630	76.8	38.1	18.73	1.38	5.19

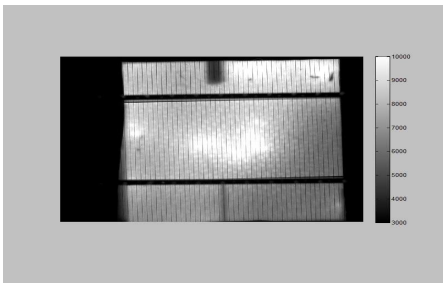

(a).

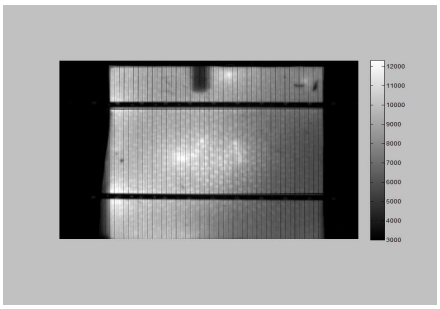

(b).

Figure 6. (a). Sample SPL-0091 3A_1min. (b). Sample SPL-00913A_1

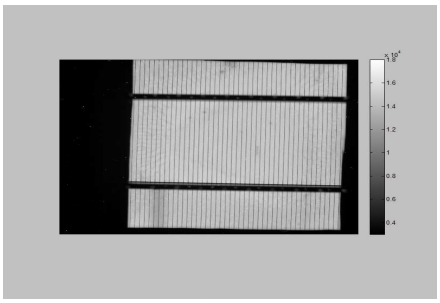

(a).

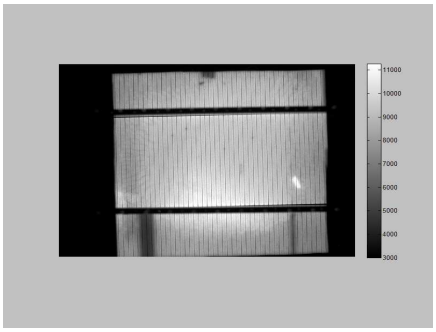

(b).

Figure 7. (a). sample SPL-0092 3A_1min., (b). Sample SPL-0092 3A_1min after FGA treatment

978-1-6654-0311-5/21/$31.00 ©2021 IEEE

Figure 6. (a). Sample SPL-0091 3A_1min.
(b). Sample SPL-00913A_1

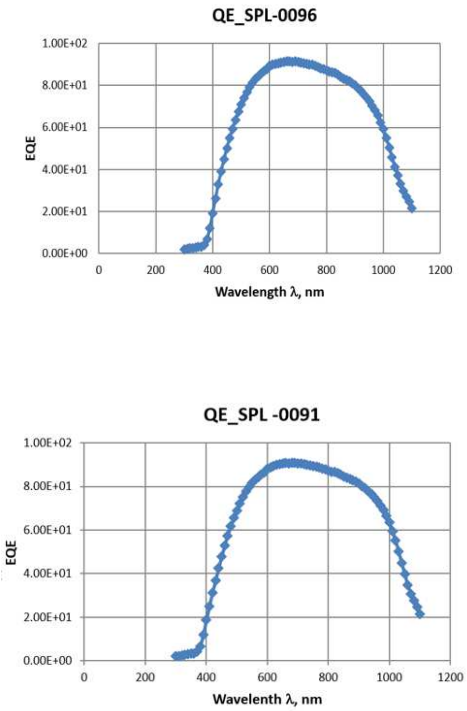

Figure 8. EQE efficiency measurement for SPL Lot15

IV. CONCLUSION

In this work, we investigated the light conversion efficiencies of Si solar cells fabricated using two types of good doping conductive Al BSF pastes, Al BSF paste from Sun Chemical and Al paste from DuPont chemicals. All the Al-BSF Si solar cells were fabricated on p-type CZ-Si substrates with resistivity of 1.0 Ω-cm, thickness of 180 µm and dimensions of 256 cm^2.

After $POCl_3$ diffusion, sheet resistance of ~640 Ω/sq was measured. Gridlines width of 45-55 µm were defined by a screen with 40 µm mesh opening. After the screen-printed metal electrodes dried, the solar cells were cofired at peak firing temperature of ~797 °C.

The best cells exhibit efficiency as high as 19.7 %, with V_{oc} of 644 mV, J_{sc} of 38. 5 mA/cm^2 and FF of 78 %.

Analysis and investigation performed during the device development and fabrication has contributed to the understanding of the local interaction between Al and Si. The Al paste readily diffuses into the Si wafer after firing. To better understand the limitations of screen-printed Al-BSF cell, various factors that affect the V_{oc}, J_{sc} and FF, as well as the conversion efficiency of a solar cell were identified. To further improve solar cell conversion efficiency, some promising front grid metallization patterns with the introduction of grid segmentation and uneven busbar needs to be investigated.

The Al/Ag firing process for the Sun Chemical product (CTX 0435) needs to be optimized as the current process disintegrates to powder substance after Ag firing.

The process window for firing the DuPont Ag front-side paste is large and yields low series resistance values without an FGA anneal. It is not clear why FGA anneal did not improve the series resistance and performance of SPL-0092 and SPL-0096.

Very good Si solar cells with external quantum efficiencies (EQE) of over 90% was measured.

REFERENCES

[1] A. Luque, S. Hegedus, Handbook of photovoltaic science and engineering, John Wiley & Sons2011.
[2] J. Hong, W. Wang, B. Shi, W. Zhang, Screen-printed Si paste for localized B doping in a back surface field, IEEE Electron Device Letters, 36 (2015) 8-10.
[3] A. Das, D.S. Kim, K. Nakayashiki, B. Rounsaville, V. Meemongkolkiat, A. Rohatgi, Boron diffusion with boric acid for high efficiency silicon solar cells, Journal of The Electrochemical Society, 157 (2010) H684-H687.
[4] Z. Wang, P. Han, H. Lu, H. Qian, L. Chen, Q. Meng, N. Tang, F. Gao, Y. Jiang, J. Wu, Advanced PERC and PERL production cells with 20.3% record efficiency for standard commercial p-type silicon wafers, Progress in Photovoltaics: Research and Applications, 20 (2012) 260-268.
[5] M. Vinodkumar, K. Korot, C. Limbachiya, B.K. Antony, Screening-corrected electron impact total and ionization cross sections for boron trifluoride (BF3) and boron trichloride (BCl3), Journal of Physics B: Atomic, Molecular and Optical Physics, 41 (2008) 245202.
[6] A. Ebong, C. Honsberg, S. Wenham, Fabrication of double sided buried contact (DSBC) silicon solar cell by simultaneous pre-deposition and diffusion of boron and phosphorus, Solar energy materials and solar cells, 44 (1996) 271-278.
[7] Y. Gao, S. Zhou, Y. Zhang, C. Dong, X. Pi, D. Yang, Doping silicon wafers with boron by use of silicon paste, Journal of Materials Science & Technology, 29 (2013) 652-654.
[8] G. Du, B. Chen, N. Chen, R. Hu, Efficient boron doping in the back surface field of crystalline silicon solar cells via alloyed-aluminum–boron paste, IEEE Electron Device Letters, 33 (2012) 573-575.
[9] S.S. Hegedus, W.N. Shafarman, Thin-film solar cells: device measurements and analysis, Progress in Photovoltaics: Research and Applications, 12 (2004) 155-176.
[10] M. Hofmann, S. Janz, C. Schmidt, S. Kambor, D. Suwito, N. Kohn, J. Rentsch, R. Preu, S.W. Glunz, Recent developments in rear-surface passivation at Fraunhofer ISE, Solar energy Materials and Solar cells, 93 (2009) 1074-1078.
[11] E. Yablonovitch, G.D. Cody, Intensity enhancement in textured optical sheets for solar cells, IEEE Transactions on Electron Devices, 29 (1982) 300-305.
[12] D. Macdonald, A. Cuevas, M.J. Kerr, C. Samundsett, D. Ruby, S. Winderbaum, A. Leo, Texturing industrial multicrystalline silicon solar cells, Solar Energy, 76 (2004) 277-283.
[13] J. Rentsch, J. Ackermann, K. Birmann, H. Furtwängler, J. Haunschild, G. Kästner, R. Neubauer, J. Nievendick, A. Oltersdorf, S. Rein, Wet chemical processing for C-Si solar cells-status and perspectives, Proceedings of the 24th European Photovoltaic Solar Energy Conference, Hamburg, Germany, 2009, pp. 1113-1117.

978-1-6654-0311-5/21/$31.00 ©2021 IEEE